

1 **Expression patterns of *Eph* genes in the “dual visual development” of**
2 **the lamprey and their significance in the evolution of vision in**
3 **vertebrates**

4
5 Daichi G. Suzuki^{a,*}, Yasunori Murakami^b, Yuji Yamazaki^c, Hiroshi Wada^a

6
7 ^aGraduate School of Life and Environmental Sciences, University of Tsukuba, Tsukuba 305-8572,
8 Japan

9 ^b Department of Biology, Faculty of Science, Ehime University, 2-5 Bunkyo-cho, Matsuyama,
10 Ehime 790-8577, Japan

11 ^c Department of Biology, Faculty of Science, Toyama University, 3190 Gofuku, Toyama 930-8555,
12 Japan

13

14 *Author for correspondence (e-mail: daichi1207@gmail.com)

15

16 **SUMMARY**

17 Image-forming vision is crucial to animals for recognizing objects in their environment. In
18 vertebrates, this type of vision is achieved with paired camera eyes and topographic projection of
19 the optic nerve. Topographic projection is established by an orthogonal gradient of axon guidance
20 molecules, such as Ephs. To explore the evolution of image-forming vision in vertebrates, lampreys,
21 which belong to the basal lineage of vertebrates, are key animals because they show unique “dual
22 visual development.” In the embryonic and pre-ammocoete larval stage (the “primary” phase),
23 photoreceptive “ocellus-like” eyes develop, but there is no retinotectal optic nerve projection. In the
24 late ammocoete larval stage (the “secondary” phase), the eyes grow and form into camera eyes, and
25 retinotectal projection is newly formed. After metamorphosis, this retinotectal projection in adult
26 lampreys is topographic, similar to that of gnathostomes. In this study, we explored the involvement
27 of *Ephs* in lamprey “dual visual development” and establishment of the image-form vision. We
28 found that gnathostome-like orthogonal gradient expression was present in the retina during the
29 “secondary” phase; i.e., *EphB* showed a gradient of expression along the dorsoventral axis, while
30 *EphC* was expressed along the anteroposterior axis. However, no orthogonal gradient expression
31 was observed during the “primary” phase. These observations suggest that *Ephs* are likely recruited
32 *de novo* for the guidance of topographical “second” optic nerve projection. Transformations during
33 lamprey “dual visual development” may represent “recapitulation” from a protochordate-like
34 ancestor to a gnathostome-like vertebrate ancestor.

35

36 INTRODUCTION

37 Image-forming vision, or object recognition, is an important sensory function that allows animals to
38 distinguish objects in the environment. In vertebrates, this type of vision evolved independently
39 from that of arthropods and cephalopods, and they have succeeded as active predators (Lacalli
40 2001). The majority of gnathostomes, the main group of vertebrates, achieve this type of vision
41 with paired camera eyes and topographic projection of the optic nerve from the retina into the
42 mesencephalic tectum. This topography is established by the orthogonal gradient of axon guidance
43 molecules, such as Ephs, and their ligands, the ephrins (Triplett and Feldheim 2012).

44 From the perspective of evolutionary biology, the evolution of image-forming vision in
45 vertebrates has attracted significant interest since it was discussed by Darwin (1859). He described
46 the vertebrate visual system as an example of extreme perfection and complication, whose
47 establishment requires overcoming the apparently imperfect intermediate stages. To understand the
48 evolutionary history of the vertebrate visual system and the intermediate stages, lampreys, which
49 belong to an ancestral group of vertebrates (cyclostomes), are key animals because they show
50 unique “dual visual development” (Suzuki et al. in press; Villar-Cheda et al. 2008; Fig. 1).

51 During the embryonic and pre-ammocoete larval stage (the “primary” phase), only a
52 simple photoreceptive “ocellus-like” eye is formed (Meléndez-Ferro et al. 2002; Villar-Cerviño et
53 al. 2006; Villar-Cheda et al. 2008). The eye of the larval lamprey is under thick and nontransparent
54 skin and has only an immature lens, suggesting that it is not an image-forming eye (Kleerekoper
55 1972). In addition, the retina of this ocellus-like eye lacks mature amacrine and horizontal cells, but
56 contains photoreceptor, ganglion, and bipolar cells (Villar-Cerviño et al. 2006). Therefore, the
57 ocellus-like eyes are thought to function as nondirectional or broadly directional photoreceptive
58 organs (Villar-Cerviño et al. 2006), although further studies are required.

59 On the other hand, the “secondary” phase corresponds to stages from late ammocoete
60 larvae to adult. During the growth of larvae, the peripheral retinal cells proliferate actively until the

61 metamorphic stage (Villar-Cheda et al. 2008), but most cells remain neuroblastic (de Miguel et al.
62 1989; Villar-Cerviño et al. 2006). During metamorphosis, these neuroblasts differentiate into
63 photoreceptor, amacrine, and horizontal cells, and the lamprey eye becomes a “truly functional”,
64 “camera-type eye” in adults (Villar-Cerviño et al. 2006; Villar-Cheda et al. 2008). This camera eye
65 of adult lampreys can process well-focused color vision (Gustafsson et al. 2008).

66 Furthermore, “dual visual development” is also observed as the development of the optic
67 nerve projection (Fig. 1). During the “primary” phase, the optic nerve projects not to the
68 mesencephalic tectum but to the prosencephalic pretectum, indicating that the visual system in this
69 “primary” phase shows primitive states as an early vertebrate (Suzuki et al. in press). The
70 retinotectal projection develops in older, larger larvae just prior to metamorphosis (de Miguel et al.
71 1990). Similar to gnathostomes, the retinotectal projection of adult lampreys occurs in a
72 topographic manner (Jones et al. 2009).

73 In the present study, we explored the involvement of *Ephs* in lamprey “dual visual
74 development” and establishment of the image-form vision. We first examined whether *Ephs* are
75 involved in the secondary phase to build topographic projections based on their gradient expression.
76 We also examined *Eph* expression during the primary phase to determine whether we can observe
77 any intermediate commitment of *Ephs* during development of the visual system.

78

79 **Materials and Methods**

80 **Animals**

81 We used *Lethenteron camtschaticum* (synonym *L. japonicum*) specimens for embryos and pre-
82 ammocoete larvae. Adult lampreys were collected in the Shiribeshi-Toshibetsu River, Hokkaido,
83 Japan. Mature eggs were squeezed from females and fertilized *in vitro* with sperm. The eggs of
84 some of the females were anesthetized in ethyl 3-aminobenzoate methanesulfonate (MS-222).
85 Embryos were cultured at 16°C. Developmental stages were determined according to Tahara (1988).
86 Since ammocoete larvae were not readily available for *L. camtschaticum*, we used *Lethenteron* sp.
87 N, the cryptic species of *L. reissneri* (Yamazaki and Goto 1998; Yamazaki et al. 2006), for late
88 stage ammocoete larvae. Ammocoete larvae were collected in the Kamo River, Upper Shougawa
89 River, Toyama, Japan, in September.

90

91 **Isolation of cDNA clones of *Eph* genes**

92 *Eph* lamprey homologs were isolated by polymerase chain reaction (PCR) using *L. camtschaticum*
93 stage 24–26 embryo cDNA as template. Primers for PCR were designed based on the *Eph* gene
94 sequences of *L. reissneri* (*LrEphB*: AB025542, *LrEphC*: AB025543), which were previously cloned
95 (Suga et al. 1999). The following primers were used:

96 *LcEphB*-F: 5'-GAGATGGCGGTCGCCATCAAGACGCTAAA-3'

97 *LcEphB*-R: 5'-TTCTTCTGGTGTCCAGCCAGGGTAACTCC-3'

98 *LcEphC*-F: 5'-AAGACTCTGAAGGCCGGGTACAGCGAGAA-3'

99 *LcEphC*-R: 5'-TGCAGGTCTTCCGGTGTTCATCTGTGCGAC-3'

100 The amino acid sequences of the isolated clones were almost identical to *LrEphB* and *LrEphC*,
101 respectively, and therefore were named *LcEphB* and *LcEphC* (*Lethenteron camtschaticum EphB*
102 and *EphC*; Acc. Nos: AB697185 and AB710343, respectively).

103

104 **Phylogenetic analysis**

105 The sequences were aligned using MAFFT (Kato and Toh 2008) and trimmed using trimAL (gap
106 threshold of 50%; Capella-Gutiérrez et al. 2009). Maximum likelihood (ML) trees were inferred
107 using RAxML 7.2.7 and the best-fitting amino acid substitution model, as determined using the
108 RAxML amino acid substitution model selection Perl script (Stamatakis 2006; Stamatakis et al.
109 2008). Confidence values of the phylogenetic trees were calculated by bootstrapping 1,000 times.

110

111 **Whole-mount and sectioning for *in situ* hybridization**

112 Whole-mount *in situ* hybridization was performed according to Ogasawara et al. (2000) with minor
113 modifications. Cryosectioning was performed on specimens embedded in Optimal Cutting
114 Temperature (O.C.T.) compound using a CM3050 III (Leica). After washing out the compounds, *in*
115 *situ* hybridization for cryosectioned materials was performed following the protocol for whole-
116 mount *in situ* hybridization, except that Tween 20 detergent was not used in any step and proteinase
117 treatment was omitted before hybridization. Densitometric scans were performed using ImageJ
118 software. As the retinas were not straight on the sectioned image, densitometry was performed after
119 gray-scale conversion and after splitting the retina into four regions using a computational graphics
120 editor (Photoshop CS6).

121

122 **Results**

123 ***Eph* genes in lampreys**

124 Previously, two lamprey *Eph* genes were isolated by Suga et al. (1999), and one was annotated as
125 an orthologue of *EphB*, because it showed a clear affinity to gnathostome *EphB*. The orthology of
126 the second gene was not clear, because it did not show obvious affinity with *EphA* and thus was
127 designated as *EphC*.

128 In a search of the *Petromyzon marinus* genome (see also Smith et al. 2013), we retrieved
129 eight gene models. However, these gene models should be used with caution, because the lamprey
130 genome is degenerated somatically (Smith et al. 2009; 2012). Thus, this does not necessarily
131 indicate that *Petromyzon* possesses eight *Eph* genes. Phylogenetic analysis showed that three *Eph*
132 genes showed affinities to *EphC*, two to Hagfish *EphA*, and three to cyclostome *EphB* (Fig. 2).
133 Among those related to *EphA*, two gene models shared a highly conserved region (approximately
134 600 bp), including a 100% matching region (200 bp). This region also displayed the same exon
135 structure. Thus, it remains possible that they represent alleles of a single gene. Similarly, three gene
136 models of *EphC* shared three highly conserved regions (approximately 330 bp, 180 bp, and 500 bp,
137 respectively), with the same exon-intron structure. Thus, they may represent alleles or products of
138 alternative splicing or products of genome rearrangement during early embryogenesis (Smith et al.
139 2009; 2012). Among the *EphB* gene models, two (*PmEphB1* and *PmEphB2*) contain partial
140 sequences with no overlap. Thus, they may originate from a single gene.

141 Although Suga et al. (1999) annotated Hagfish *EphA* as cognates of gnathostome *EphAs*,
142 the orthology among cyclostome *EphA*, *EphC* and gnathostome *EphAs* remains unclear (Fig. 2). It
143 should be noted that common expression patterns were observed between lamprey *EphC* and
144 gnathostomes *EphAs*, specifically in rhombomeres 3 and 5 (r3 and r5, respectively), suggestive of
145 their evolutionary affinity (Murakami et al. 2004; 2005).

146 From the transcripts of embryos (stages 25 and 26) and ammocoete larvae (10 cm long),

147 we isolated two *Eph* genes (*EphB* and *EphC*) from *L. camtschaticum*. However, *EphA* transcripts
148 could not be isolated from either stage, suggesting that *EphA* genes were not expressed, or that its
149 expression was low during the stages examined. Thus, we analyzed the expression patterns of *EphB*
150 and *EphC*.

151

152 **Expression patterns of Eph genes in late ammocoete larvae: the “secondary” phase**

153 In gnathostomes, *EphB* genes show a gradient of expression along the dorsoventral axis with higher
154 expression ventrally in the retina. However, *EphB* does not show an obvious gradient in the
155 mediolateral axis of the tectum (Triplett and Feldheim 2012). *EphA* genes also showed gradient
156 expression, but along the anteroposterior axis with higher levels in the temporal/posterior regions of
157 the retina and in the anterior of the tectum (Triplett and Feldheim 2012).

158 We examined the expression of *Eph* genes in late ammocoete larvae of approximately 90–
159 130 mm long. At this size, larvae are in the “secondary” phase when the retinotectal optic
160 projection is established. de Miguel et al. (1990) reported that ammocoete larvae longer than 70–80
161 mm already show retinotectal projection in *Petromyzon marinus* and *Lampetra fluviatilis*.

162 In the retina of late ammocoete larvae, *EphB* expression was detected in a gradient manner
163 along the dorsoventral axis with higher expression ventrally (Fig. 3A). We detected this gradient
164 expression reproducibly in all four specimens (for other specimen samples, see Supplementary Fig.
165 S1) and confirmed it by densitometric analysis (Fig. S2). On the other hand, we did not detect
166 reproducible gradient patterns along the anteroposterior axis (Fig. 3C). We also detected gradient
167 expression of *EphC*, but along the anteroposterior axis with higher expression posteriorly (Fig. 3D).
168 In addition, this gradient was observed reproducibly in all four specimens examined, which was
169 confirmed based on densitometric analysis (for example, see Supplementary Fig. S1 and Fig. S2).
170 However, we did not observe gradient expression along the dorsoventral axis for *EphC* (Fig. 3B).

171 The tectum of lampreys can be divided into the superficial and deeper layers. The optic

172 nerve axons terminate in this superficial layer (Kosareva 1980). Based on expression analysis, both
173 *EphB* and *EphC* showed wide and strong expression in the inner layer of the brain. However,
174 expression in the superficial layer was restricted to the tectum and was not observed in the
175 surrounding brain region (Fig. 5, A–D). These expression patterns suggested that Ephs functions as
176 axon guidance molecules. However, our observations did not reveal any expression gradients in the
177 tectum, possibly because of technical limitations in detecting subtle differences in expression levels
178 in sectioned materials.

179

180 **Expression patterns of *Eph* genes in embryos and pre-ammocoete larvae: the “primary”**
181 **phase**

182 Our analyses in the “secondary phase” revealed an orthogonal gradient of *Ephs*, at least in the retina.
183 Based on these results, we next explored whether a similar pattern was observed during the
184 “primary” phase. As reported by Suzuki et al. (in press), the “primary” optic nerve formed after
185 stage 25 and projected to the pretectum. This projection pattern may represent ancestral visual
186 systems, because similar neuroarchitectures were observed in amphioxus. Thus, the primary visual
187 system of lampreys provides a unique system to assess the evolutionary history of *Eph* gene
188 commitment in the visual system. Thus, we examined the expression patterns of *Eph* genes during
189 development of the “primary” optic nerve from ocellus-like eyes in pre-ammocoete larvae.

190 The expression of *EphB* was observed as early as stage 24 in the presumptive
191 diencephalic–rhombencephalic brain, as well as in the upper and lower lips (Fig. 6A). The
192 expression levels in the brain increased at stage 25, especially in the anterodorsal thalamus (Fig.
193 6B). At stage 26, *EphB* expression was detected widely in the brain throughout the diencephalon
194 (thalamus, pineal organ, pretectum, and diencephalic tegmentum), mesencephalon, and
195 rhombencephalon (Fig. 6C), but no gradient expression was observed in the tectum or pretectum,
196 the presumptive target for the “primary” optic nerve at this stage (white broken line). In addition, no

197 signal was observed in the eyeball (eb) (Fig. 6D). After stage 27 (Fig. 6E), *EphB* expression
198 decreased, but was still detected in the anterodorsal thalamus, mesencephalon, and
199 rhombencephalon, as well as in the upper and lower lips and branchial arches.

200 The expression of *EphC* was detected slightly earlier than *EphB* from stage 23 in the
201 forebrain (fb), r3 and r5, and the trigeminal ganglion (gV; Fig. 7A). At stage 24, expression in the
202 forebrain was restricted to the dorsalmost telencephalon, dorsalmost thalamus, and ventral
203 diencephalic tegmentum (tg). It was also expressed in the facial ganglion (gVII) and weakly in
204 rhombomere 6 (r6), as well as the upper and lower lips, somites (sm), and branchial arches (ba; Fig.
205 7B, B'). At stage 25, expression in the dorsal telencephalon and the anterodorsal thalamus increased.
206 In addition, expression was detected in the eyeball (Fig. 7C). During this stage, *EphC* expression
207 was still observed in the rhombomeres (r3 and r5), as reported previously (Murakami et al. 2004).
208 At stage 26, we detected *EphC* expression in the optic stalk, eyeball, and the otic vesicle (otv). Note
209 that in the eyeball, the expression was stronger in the marginal zone (Fig. 7D, E). Expression was
210 also detected in the pretectum, which contained the presumptive "primary" optic nerve (Fig. 4D',
211 white broken line), but no gradient was observed and instead was present in a uniform manner. The
212 expression of *EphC* clearly decreased after stage 27 (Fig. 7F, G).

213

214 **Discussion**

215 **Establishment of image-forming vision in lampreys**

216 Topography of the retinotectal projection is formed by the orthogonal gradient of axon guidance
217 molecules such as Ephs and ephrins, which forms the basis for image-forming vision in
218 gnathostomes (Triplett and Feldheim 2012).

219 We found that during the “secondary” phase of lamprey dual visual development, the
220 expression patterns of *Eph* genes showed a gnathostome-like orthogonal gradient in the retina.
221 These gradient patterns were similar to those in gnathostomes; *EphB* showed a gradient of
222 expression along the dorsoventral axis with higher expression ventrally. In addition, *EphC* showed a
223 gradient of expression along the anteroposterior axis with higher expression posteriorly, which was
224 similar to the pattern of gnathostome *EphA*. These results indicate that the topography of the
225 “secondary” phase optic nerve in lampreys is formed by an axon guidance system similar to that of
226 gnathostomes. However, the expression gradients of these genes in the tectum remains unclear,
227 possibly due to technical difficulties in detecting fine quantitative differences in expression levels in
228 sectioned materials. Alternatively, the *Eph* gradient in the retina and *ephrin* gradient in the tectum
229 may be sufficient for the development of the lamprey topographic visual system, although it was
230 difficult to detect the expression of *ephrin* genes due to their short transcript lengths. In addition, we
231 could not isolate any *EphA* transcripts in embryos or ammocoete larvae, indicating that *EphA* genes
232 are expressed at low levels during these stages. However, the common expression patterns between
233 Lamprey *EphC* and gnathostomes *EphAs*, not only in rhombomeres 3 and 5 but also in the gradient
234 manner in retina observed in this study, suggests that they are evolutionary favored compared with
235 cyclostome *EphAs*.

236 Despite these issues, the clear gradients of *Eph* gene expression in the retina were
237 consistent with previous observations that the retinotectal optic nerve projection forms during the
238 late larval stage just prior to metamorphosis (de Miguel et al. 1990) and that the retinotectal optic

239 nerve projection in adults is topographic (Jones et al. 2009). Therefore, our results support the
240 hypothesis that the “secondary” optic nerve topography may be mediated by the orthogonal gradient
241 of axon guidance molecules, such as Ephs.

242

243 **“Dual visual development” of lampreys and its evolutionary significance in vertebrates**

244 Suzuki et al. (in press) reported that the “primary” optic nerve projects not to the tectum, but to the
245 pretectum, and the “primary” visual system may represent an ancestral state comparable with that of
246 the amphioxus. Thus, we can assess the following scenarios for the evolutionary history of *Eph* and
247 the visual system. First, if the orthogonal gradient is observed in the retina and tectum during the
248 primary optic nerve projection, the *Eph* gradient may be primarily established not for the visual
249 system, but for some other neuroanatomical development, and this system was secondarily exapted
250 for topographical projection. Second, if the orthogonal gradient is observed in the retina and
251 pretectum during primary optic nerve projection, the *Eph* gradient is likely involved in the nerve
252 projection of the primary visual system. This further suggests that the primary visual system may be
253 topographical. Third, in cases of *Eph* expression specifically in the retina and pretectum (but
254 without gradient), *Eph* may be involved in optic nerve projection. However, this optic nerve
255 projection likely is not topographical. Finally, if specific expression of *Ephs* is not observed in the
256 retina or pretectum, *Ephs* are more likely to be recruited *de novo* for the guidance of topographical
257 “second” optic nerve projection.

258 Our results showed that the expression patterns of *Eph* genes differed during the “primary”
259 phase from those in gnathostomes or during the “secondary” phase of the lamprey. *EphB* expression
260 was not detected in the eyeball. Although both *EphB* and *EphC* expression was detected in the
261 target brain regions of the “primary” optic nerve, the expression was observed widely in the
262 diencephalon and not confined to the specific target region. Furthermore, in the tectum, *EphB*
263 expression did not show gradient expression but instead was observed in a uniform manner. *EphC*

264 was not expressed in the tectum. Thus, neither *EphB* nor *EphC* show gnathostome-like orthogonal
265 gradients in the eyeball, the “primary” visual center or the tectum.

266 These observations did not support the first or second scenarios, because no orthogonal
267 gradient was observed in the retina or tectum. Because the expression of *EphB* and *EphC* did not
268 respect the boundary of the pretectum or tectum, our results favor the final scenario that *Ephs* were
269 recruited *de novo* for the guidance of topographical “second” optic nerve projection. However, it
270 remains possible that *Ephs* are involved in axon guidance of the “primary” optic nerve. In addition,
271 strong expression was observed for *EphC* in the margin of the eyeball of stage 26 larvae (Fig. 4D,
272 E), which may suggest that lamprey *EphC* is involved in the development of the eyeball in a unique
273 manner.

274 Similar to their “dual visual development”, lampreys show remarkable transformation
275 during metamorphosis from a protochordate-type character status to a vertebrate-type status. For
276 example, the endostyle in the larval stage transforms into the thyroid gland during metamorphosis
277 (Wright et al. 1980). In addition, no arcualia (vertebral rudiments) are observed in the larval stage,
278 but they appear after metamorphosis (Potter and Welsch 1992; Richardson et al. 2010). From an
279 evolutionary perspective, these transformations may represent “recapitulation” from a
280 protochordate-like ancestor to a gnathostome-like vertebrate ancestor. Further studies on the
281 developmental transition from the larval to adult type may provide insights into the evolution of
282 vertebrate-specific characters, such as image-forming vision.

283

284 **ACKNOWLEDGEMENTS**

285 The authors thank the anonymous reviewers for their constructive comments and suggestions that
286 improved the quality of the article. This work is supported by Grant-in-Aid for JSPS Fellows
287 13J00621 to D.G.S., and Grant-in-Aid for Scientific Research on Innovative Areas 23128502 to
288 H.W.

289

290 **REFERENCES**

- 291 Capella-Gutiérrez, S., Silla-Martínez, J. M., and Gabaldón, T. 2009. trimAl: a tool for automated
292 alignment trimming in large-scale phylogenetic analyses. *Bioinformatics* 25: 1972–1973.
- 293 Darwin, C. 1859. *On the Origin of Species*. John Murray, London.
- 294 Gustafsson, O. S. E., Collin, S. P., and Kröger, R. H. H. 2008. Early evolution of multifocal optics
295 for well-focused colour vision in vertebrates. *J. Exp. Biol.* 211: 1559–1564.
- 296 Jones, M. R., Grillner, S., and Robertson, B. 2009. Selective projection patterns from subtypes of
297 retinal ganglion cells to tectum and pretectum: distribution and relation to behavior. *J. Comp.*
298 *Neurol.* 517: 257–275.
- 299 Katoh, K., and Toh, H. 2008. Recent developments in the MAFFT multiple sequence alignment
300 program. *Briefings Bioinfo.* 9: 286–298.
- 301 Kleerekoper, H. 1972. The sense organs. In M. W. Hardisty and I. C. Potter (eds.). *The Biology of*
302 *Lampreys*, vol 2, Academic Press, London. pp. 373–404.
- 303 Kosareva, A. A. 1980. Retinal projections in lamprey (*Lampetra fluviatilis*). *J. Hirnforsch.* 21: 243–
304 256.
- 305 Lacalli, T. C. 2001. New perspectives on the evolution of protochordate sensory and locomotory
306 systems, and the origin of brains and heads. *Phil. Trans. R. Soc. Lond. B* 356: 1565–1572.
- 307 Meléndez-Ferro, M., Villar-Cheda, B., Abalo, X. -M., Pérez-Costas, E., Rodríguez-Muñoz, R.,

308 Degrip, W. J., Yáñez, J., Rodicio, M. C., and Anadón, R. 2002. Early development of the retina
309 and pineal complex in the sea lamprey: comparative immunocytochemical study. *J. Comp.*
310 *Neurol.* 442: 250–265.

311 Murakami, Y., Pasqualetti, M., Tako, Y., Hirano, S., Rijili, F. M., and Kuratani, S. 2004. Segmental
312 development of reticulospinal and branchiomotor neurons in lamprey: insights into the
313 evolution of the vertebrate hindbrain. *Development* 131: 983–995.

314 Murakami, Y., Uchida, K., Rijili, F. M., and Kuratani, S. 2005. Evolution of the brain
315 developmental plan: Insights from agnathans. *Dev. Biol.* 280: 249–259.

316 de Miguel, E., Rodicio, M. C., and Anadón, R. 1989. Ganglion cells and retinopetal fibers of the
317 larval lamprey retina: an HRP ultrastructural study. *Neurosci. Lett.* 106: 1–6.

318 de Miguel, E., Rodicio, M. C., and Anadón, R. 1990. Organization of the visual system in larval
319 lampreys: an HRP study. *J. Comp. Neurol.* 302: 529–542.

320 Ogasawara, M., Shigetani, Y., Hirano, S., Satoh, N., and Kuratani, S. 2000. *Pax1/Pax9*-related
321 genes in an agnathan vertebrate, *Lampetra japonica*: expression pattern of *LjPax9* implies
322 sequential evolutionary events toward the gnathostome body plan. *Dev. Biol.* 223: 399–410.

323 Potter, I. C., and Welsch, U. 1992. Arrangement, histochemistry and fine structure of the connective
324 tissue architecture of lampreys. *J. Zool.* 225: 1–30.

325 Richardson, M. K., Admiraal, J., and Wright, G. M. 2010. Developmental anatomy of lampreys.
326 *Biol. Rev.* 85: 1–33.

327 Stamatakis, A. 2006. RAxML-VI-HPC: Maximum Likelihood-based Phylogenetic Analyses with
328 Thousands of Taxa and Mixed Models. *Bioinformatics* 22: 2688–2690.

329 Stamatakis, A., Hoover, P., and Rougemont, J. 2008. A Rapid Bootstrap Algorithm for the RAxML
330 Web-Servers. *Syst Biol.* 57: 758–771.

331 Suga, H., Hoshiyama, D., Kuraku, S., Katoh, K., Kubokawa, K., and Miyata, T. 1999. Protein
332 tyrosine kinase cDNAs from amphioxus, hagfish, and lamprey: isoform duplications around the

333 divergence of cyclostomes and gnathostomes. *J. Mol. Evol.* 49: 601–608.

334 Smith, J. J., Kuraku, S., Holt, C., Sauka-Spengler, T., Jiang, N., Campbell, M. S., Yandell, M. D.,
335 Manousaki, T., Meyer, A., Bloom, O. E., Morgan, J. R., Buxbaum, J. D., Sachidanandam, R.,
336 Sims, C., Garruss, A. S., Cook, M., Krumlauf, R., Wiedemann, L. M., Sower, S. A., Decatur,
337 W. A., Hall, J. A., Amemiya, C. T., Saha, N. R., Buckley, K. M., Rast, J. P., Das, S., Hirano,
338 M., McCurley, N., Guo, P., Rohner, N., Tabin, C. J., Piccinelli, P., Elgar, G., Ruffier, M., Aken,
339 B. L., Searle, S. M., Muffato, M., Pignatelli, M., Herrero, J., Jones, M., Brown, C. T., Chung-
340 Davidson, Y. W., Nanlohy, K. G., Libants, S. V., Yeh, C. Y., McCauley, D. W., Langeland, J.
341 A., Pancer, Z., Fritsch, B., de Jong, P. J., Zhu, B., Fulton, L. L., Theising, B., Flicek, P.,
342 Bronner, M. E., Warren, W. C., Clifton, S. W., Wilson, R. K., and Li, W. 2013. Sequencing of
343 the sea lamprey (*Petromyzon marinus*) genome provides insights into vertebrate evolution. *Nat.*
344 *Genet.* 45: 415–421.

345 Smith, J. J., Antonacci, F., Eichler, E. E. and Amemiya, C. T. 2009. Programmed loss of millions of
346 base pairs from a vertebrate genome. *Proc. Natl. Acad. Sci. USA* 106: 11212–11217.

347 Smith, J. J., Baker, C., Eichler, E. E. and Amemiya, C. T. 2012. Genetic consequences of
348 programmed genome rearrangement. *Curr. Biol.* 22: 1524–1529.

349 Suzuki D. G., Murakami, Y., Escriva, H., and Wada, H. in press. A comparative examination of
350 neural circuit and brain patterning between the lamprey and amphioxus reveals the
351 evolutionary origin of the vertebrate visual center. *J. Comp. Neurol.*

352 Tahara, Y. 1988. Normal stages of development in the lamprey, *Lampetra reissneri* (Dybowski).
353 *Zool. Sci.* 5: 109–118.

354 Triplett, J. W., and Feldheim, D. A. 2012. Eph and ephrin signaling in the formation of topographic
355 maps. *Semin. Cell Dev. Biol.* 23: 7–15.

356 Villar-Cerviño, V., Abalo, X. -M., Villar-Cheda, B., Meléndez-Ferro, M., Pérez-Costas, E.,
357 Horstein, G. R., Martinelli, G. P., Rodicio, M. C., and Anadón, R. 2006. Presence of glutamate,

358 glycine, and aminobutyric acid in the retina of the larval sea lamprey: comparative
359 immunohistochemical study of classical neurotransmitters in larval and postmetamorphic
360 retinas. *J. Comp. Neurol.* 499: 810–827.

361 Villar-Cheda, B., Abalo, X. -M., Villar-Cerviño, V., Barreiro-Iglesias, A., Anadón, R., and Rodicio,
362 M. C. 2008. Late proliferation and photoreceptor differentiation in the transforming lamprey
363 retina. *Brain Res.* 1201:60–67.

364 Wright, G. M., Filisa, M. F., and Youson, J. H. 1980. Immunocytochemical localization of
365 thyroglobulin in the transforming endostyle of anadromous sea lampreys, *Petromyzon marinus*
366 L., during metamorphosis. *Gen. Comp. Endocr.* 42: 187–194.

367 Yamazaki, Y., and Goto, A. 1998. Genetic structure and differentiation of four *Lethenteron* taxa
368 from the Far East, detected from allozyme analysis. *Env. Biol. Fish* 52: 149–161.

369 Yamazaki, Y., Yokoyama, R., Nishida, M., and Goto, A. 2006. Taxonomy and molecular
370 phylogeny of *Lethenteron* lampreys in eastern Eurasia. *J. Fish Biol.* 68: 251–269.

371

372 **Figure Legends**

373 **Fig. 1.** Schematic diagram of “dual visual development,” adapted from de Miguel et al. (1990),
374 Jones et al. (2009), Meléndez-Ferro et al. (2002), Suzuki et al. (in press) and Villar-Cheda et al.
375 (2008). By the pre-ammocoete larval stage, the eyeball (eb) and optic stalk (os) are formed by
376 evagination of the brain. The lens (ls) is flattened and the retina (R) is small. The “primary” optic
377 nerve (ON¹) projects into the pretectum, and not to the tectum (tc). According to larval growth, the
378 eyes grow again by proliferation of the peripheral (lateral) retina. During the late ammocoete stage,
379 the newly developed “secondary” optic nerve (ON²) projects to the tectum. In the lateral retina,
380 neuroblastic cells (NbCs) remain undifferentiated, except retinal ganglion cells and their optic nerve
381 fibers. In the central retina (CR), photoreceptor cells are already differentiated. After
382 metamorphosis, in the adult, the retinotectal optic nerve projection is topographic, and NbCs are
383 differentiated. Abbreviations: eb, eyeball; ls, lens; NbCs, neuroblastic cells; ON¹, “primary” optic
384 nerve; ON², “secondary” optic nerve; os, optic stalk; R, retina; tc, tectum.

385

386 **Fig. 2.** Molecular phylogenetic tree for Eph genes. The tree was constructed using the ML method.
387 The numbers at the nodes represent bootstrap values. Lc: *L. camtschaticum*, Lr: *L. reissneri*, Pm: *P.*
388 *marinus*.

389

390 **Fig. 3.** Sections of *in situ* hybridization in late ammocoete larvae of lampreys (*L. sp. N*) in the retina.
391 (A, B) In transverse sections of the retina, a gradient of *EphB* expression was observed along the
392 dorsoventral axis with strong expression ventrally (arrow). In contrast, *EphC* showed uniform
393 expression. (C, D) In horizontal sections, while *EphB* showed uniform expression, a gradient of
394 *EphC* expression was observed along the anteroposterior axis with stronger expression posteriorly
395 (arrow). Abbreviations: di, diencephalon; tc, tectum; tg tegmentum. Scale bar: 200 μm.

396

397 **Fig. 4.** Densitometric scan on the *EphB* and *EphC* expression patterns in the retina of the late
398 ammocoete larvae shown in Fig. 5. The scan is performed after gray-scale conversion, cutting
399 region by region along the retina (boxes in A1, B1, C1 and D1) and linearization. The results of the
400 scan are shown in A2, B2, C2 and D2, respectively. (A, B) Transverse sections. (A) *EphB*. (B)
401 *EphC*. (C, D) Horizontal sections. (C) *EphB*. (D) *EphC*.

402

403 **Fig. 5.** Sections of *in situ* hybridization in late ammocoete larvae of lampreys (*L* sp. N) in the
404 tectum. (A, B) In transverse sections of the tectum, both *EphB* and *EphC* showed uniform
405 expression in the inner layer of the tectum and tegmentum. In the superficial layer, the expression
406 was restricted to the tectum, but no clear gradient of expression was observed. (C, D) In horizontal
407 sections, *EphB* and *EphC* expression was observed in the inner layer of the tectum and
408 diencephalon. However, expression in the superficial layer was restricted to the tectum. Broken
409 lines indicate the border of the tectum in the superficial layer and asterisks indicate the border of the
410 tectum in the deep layer. Abbreviations: di, diencephalon; tc, tectum; tg tegmentum. Scale bar: 200
411 μm .

412

413 **Fig. 6.** Whole-mount *in situ* hybridization of *EphB* in lamprey embryos and pre-ammocoete larvae
414 (*L. camtschaticum*). White broken lines indicate the dorsocaudal thalamus and pretectum region,
415 which is the presumptive target region of “primary” optic nerves. At stages (A) 24, (B) 25, and (C)
416 26. (D) In a transverse section at the level of the eyeball (eb) at stage 26 and (E) stage 27.
417 Abbreviations: ba, branchial arches; eb, eyeball; es, endostyle; ll, lower lip; mes, mesencephalon;
418 MHB, mid-hindbrain boundary; po, pineal organ; rho, rhombencephalon; th, thalamus. Scale bar:
419 200 μm .

420

421 **Fig. 7.** Whole-mount *in situ* hybridization of *EphC* in lamprey embryos and pre-ammocoete larvae
422 (*L. camtschaticum*). White broken lines indicate the presumptive dorsocaudal thalamus and
423 pretectum region, the location of the “primary” optic nerve projecting region. (A) At stage 23. (B)
424 At stage 24, the craniofacial region. (B) At stage 24, the whole embryo. At stages (C) 25 and (D) 26.
425 (D’) The same specimen as (D) focused on the brain. (E) Transverse section at the eb level of larvae
426 at stages 26, (F) 27, and (G) 28. Abbreviations: ba, branchial arches; eb, eyeball; es, endostyle; fb,
427 forebrain; gV, trigeminal ganglion; gVII, facial ganglion; ll, lower lip; mes, mesencephalon; MHB,
428 mid–hindbrain boundary; os, optic stalk; otv, otic vesicle; rho, rhombencephalon; r3/5/6,
429 rhombomeres 3/5/6, respectively; sm, somites; tel, telencephalon; tg, tegmentum; th, thalamus.
430 Scale bars: 200 μ m in (A, B, C–G applied in A) and (B’).

431

432 **SUPPLEMENTARY MATERIAL**

433 **Supplementary Fig. 1.** Sections of other specimens used for *in situ* hybridization of the retina of
434 late ammocoete lamprey larvae (*L. sp. N*). (A–D) Transverse sections showing expression levels
435 along the dorsoventral axis of specimen 3 (A, B) and specimen 4 (C, D). (E, F) Horizontal sections
436 of specimen 5 showing expression along the anteroposterior axis. (A, C, E) *EphB* and (B, D, F)
437 *EphC*. Scale bar: 200 μ m.

438

439 **Supplementary Fig. 2.** Densitometric scan of the results shown in Fig. S1.

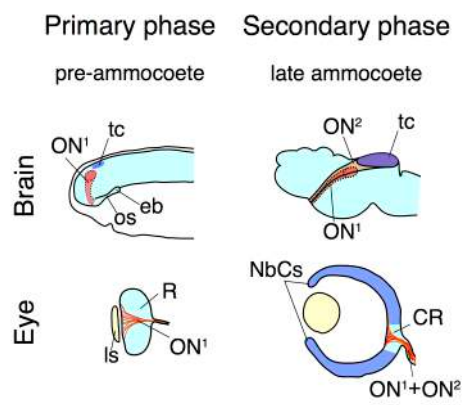


Fig. 1.

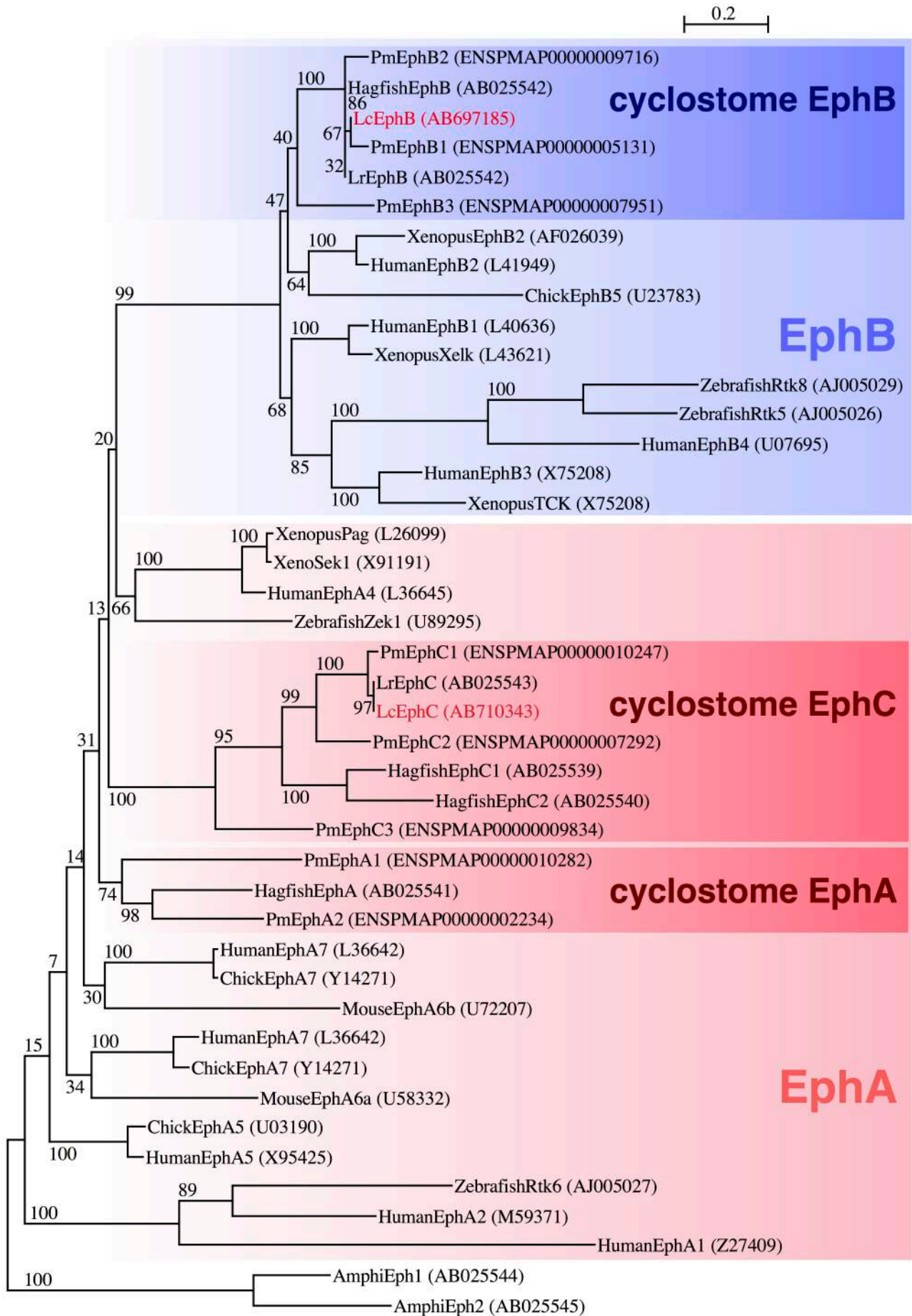


Fig. 2.

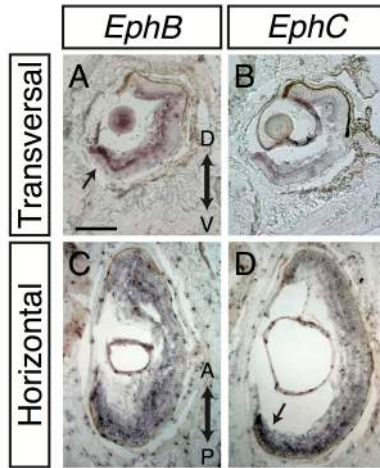


Fig. 3.

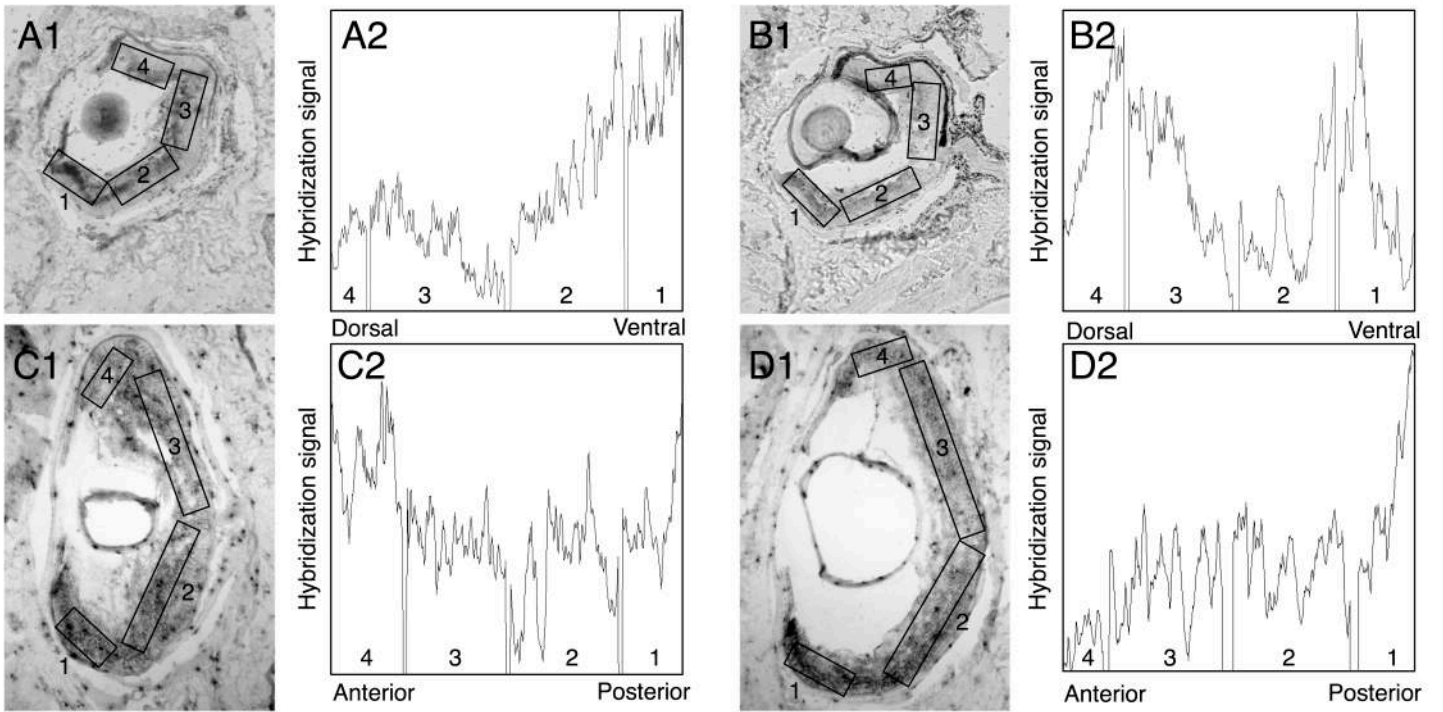


Fig. 4.

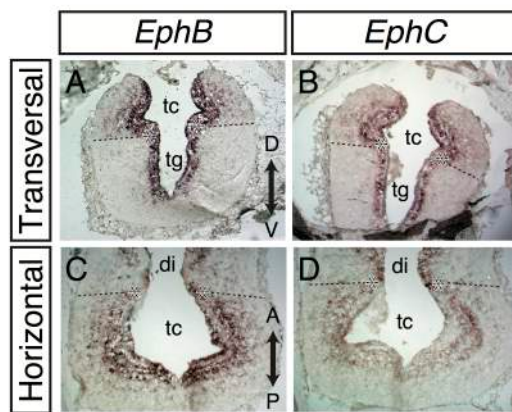


Fig. 5.

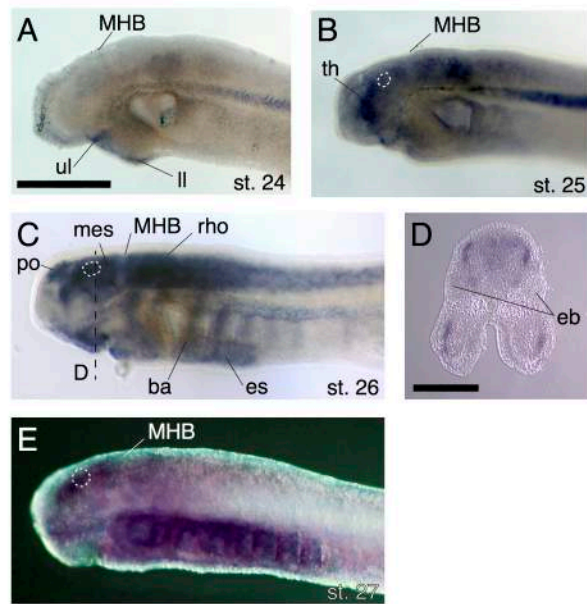


Fig. 6.

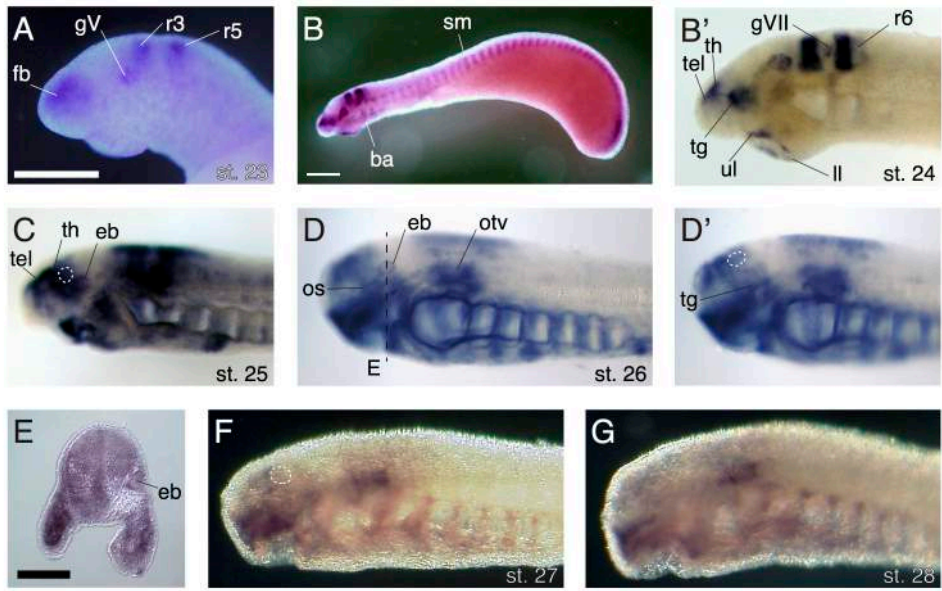


Fig. 7.

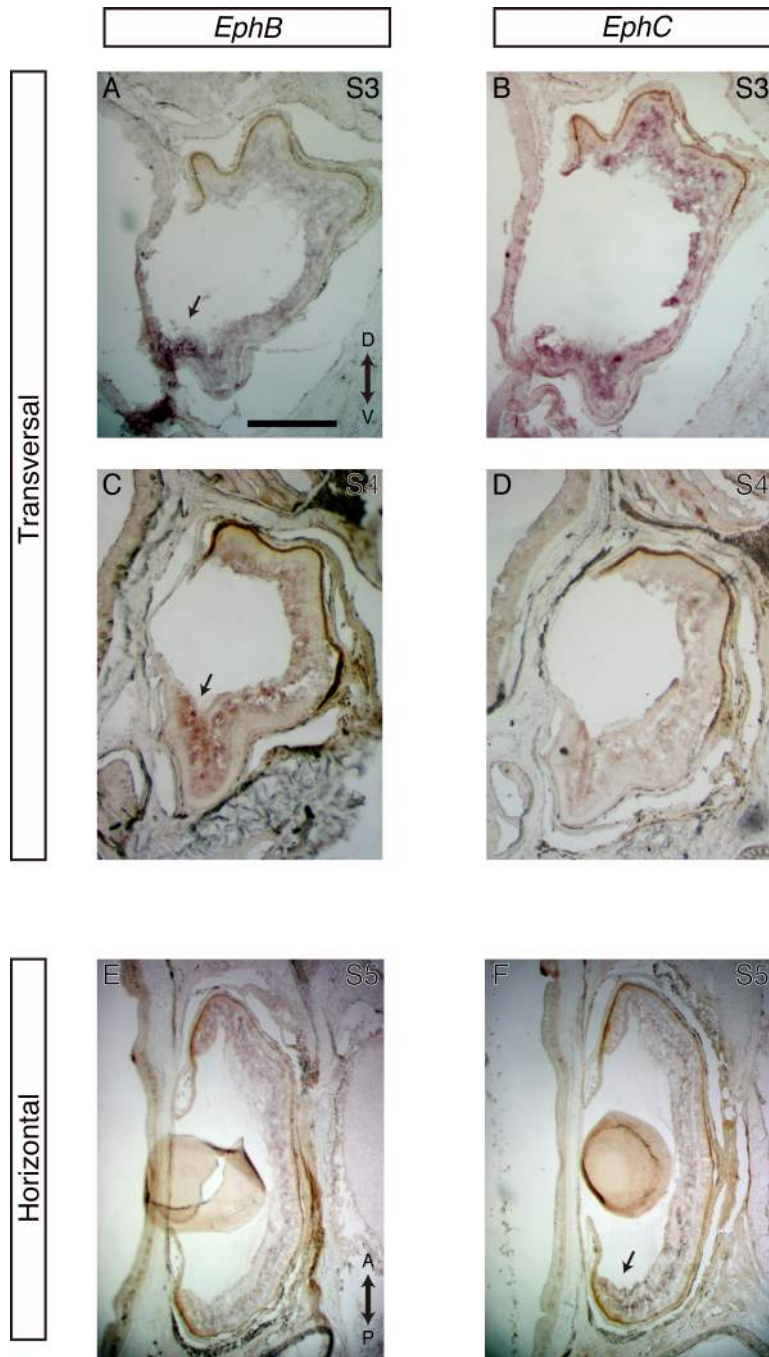


Fig S1.

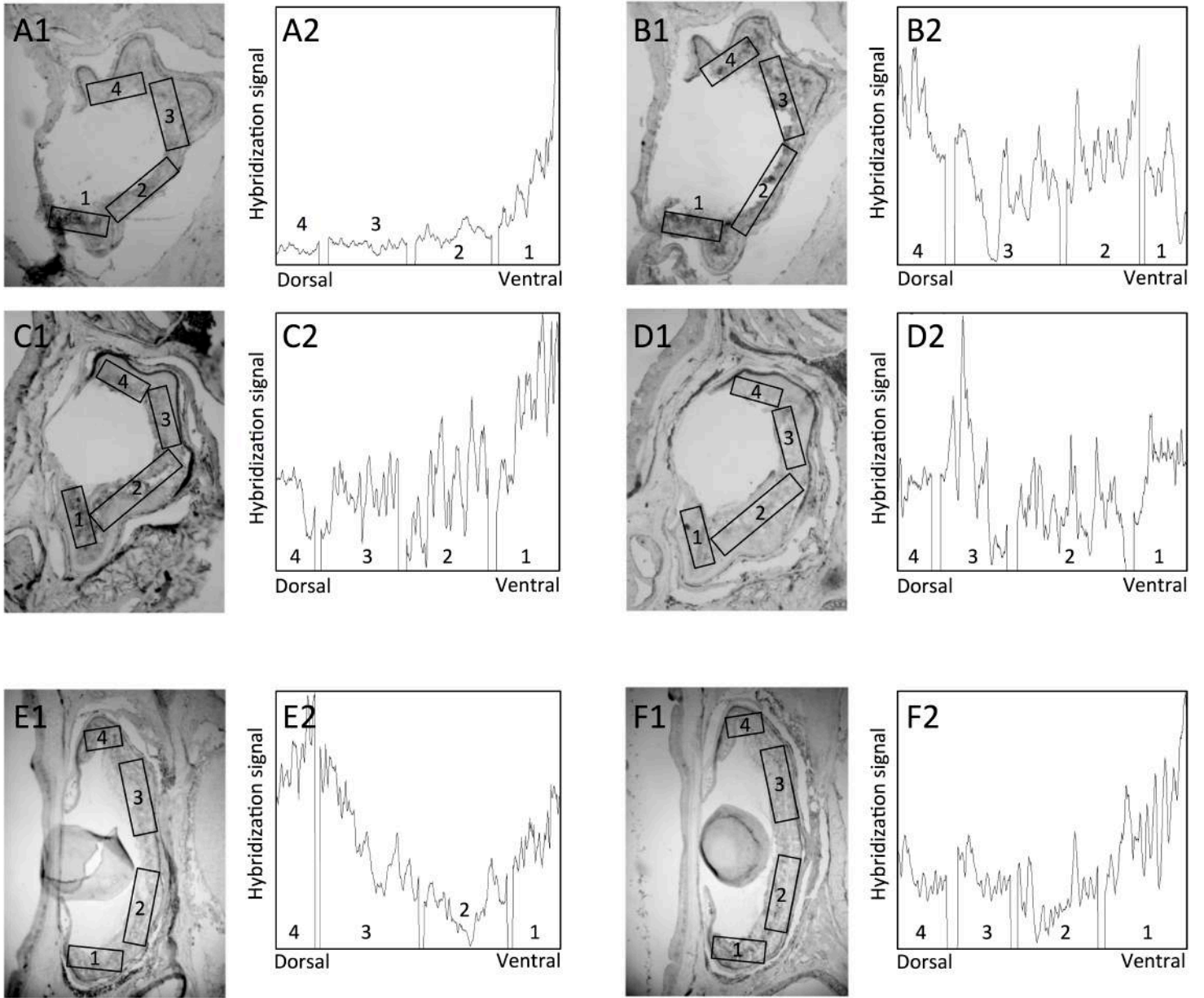


Fig S2.